Effect of grain direction on transmittance of 100-GHz millimeter wave for hinoki (Chamaecyparis obtusa)

AUTHOR(S):

Tanaka, Soichi; Fujiwara, Yuko; Fujii, Yoshihisa; Okumura, Shogo; Togo, Hiroyoshi; Kukutsu, Naoya; Nagatsuma, Tadao

CITATION:

Tanaka, Soichi ...[et al]. Effect of grain direction on transmittance of 100-GHz millimeter wave for hinoki (Chamaecyparis obtusa). Journal of Wood Science 2011, 57(3): 189-194

ISSUE DATE:

2011-06

URL:

http://hdl.handle.net/2433/143691

Original article

Title

Effect of grain direction on transmittance of 100 GHz millimeter-wave for hinoki (*Chamaecyparis obtusa*)*

Author's information

Soichi Tanaka, Yuko Fujiwara, Yoshihisa Fujii, Shogo Okumura
Graduate School of Agriculture, Kyoto University, Kyoto 606-8502, Japan

Hiroyoshi Togo, Naoya Kukutsu
NTT Microsystem Integration Laboratories, Atsugi 243-0198, Japan

and

Tadao Nagatsuma
Graduate School of engineering Science, Osaka University, Toyonaka 560-8531, Japan

Corresponding Author

Soichi Tanaka
e-mail: stanaka@h3news1.kais.kyoto-u.ac.jp
Tel. +81-75-753-6245; Fax. +81-75-753-6245

Key words

Millimeter-wave, Transmittance, Attenuation, Fiber direction, Anisotropy

* Part of this report was presented at the Annual Meeting of the Japan Wood Research Society, Tsukuba, March 2008

Abstract

The attenuation coefficients of 100 GHz millimeter-wave polarized linearly were measured for cross-cut, quarter-sawn, and flat-sawn boards of hinoki (*Chamaecyparis obtusa*) that were 0.2 to 2.0 cm thick in order to examine the applicability of free-wave propagation theory for applying electro-magnetic waves to wood. It was found that the transmittance of a millimeter wave through the specimen boards was smaller for cases where the fiber direction of a board was parallel to the direction of the electric field of the incident wave than for those where the fiber direction was perpendicular to the electric field, and there was little difference in the transmittance between the tangential and radial directions for the former case. These findings were quantitatively explainable by using the propagation theory and the dielectric properties of wood.

Introduction

The millimeter-wave technique, in which the electromagnetic waves in the frequency range of 30 to 300 GHz are used, has only recently been developed and is expected to be used for not only communications but also imaging in dielectric materials[1-5]. The millimeter-wave imaging technique can be used in the nondestructive testing of wood, and it has a higher resolution than the microwave technique which has been used for the nondestructive evaluation of wood. There have been, however, only a few basic studies[10,11] on the dielectric properties of wood in the millimeter-wave frequency range. These dielectric properties are generally characterized by their parameters such as their complex permittivity or attenuation and phase coefficients. To explain the dielectric property of orthotropic materials such as wood, these parameters need to be in three directions along the principal axes of the anisotropy are required.

In previous studies[6-9], the dielectric properties of wood have been measured by using methods in a microwave frequency range below 30 GHz:

・Detection of microwaves transmitted through the waveguides filled with wood[6,7],

・Detection of free microwave beams transmitted through and reflected in wood[8,9].

The former method is better than the latter in terms of accuracy when measuring the permittivity, because the electric field is more stable in and around the specimen in the waveguide, and the free electric field used in the latter method is often unstable because of scattering and diffraction of the microwave induced by the component of the apparatus, especially in the microwave frequency range. The latter method is preferable to the nondestructive evaluation of wood, especially when using two- or three-dimensional imaging, because the local permittivity in wood can be measured by using the latter method, while only the average permittivity of the whole specimen is obtained by the former method. In the millimeter wave frequency range, it is difficult to evaluate the dielectric properties of wood using the former method since a cross section of the waveguide, which is usually only a few millimeters square, is too small to ignore the effect of the heterogeneity of the wood, such as the annual ring structure. The latter method is, therefore, required for obtaining a more accurate evaluation of the dielectric properties of wood in the millimeter frequency range.

There have been two previous studies for the measurement of the dielectric properties of wood in the frequency ranges that include millimeter waves. Reid *et al.*[10] measured the dielectric properties of air-dried spruce in a frequency range of 100 GHz to 1.6 THz by using a teraherz pulse wave. Oyama *et al.*[11] measured the dependence of the dielectric properties of wood on its density and moisture content. They, however, did not discuss the anisotropy of the dielectric properties of the wood.

For the anisotropy of the dielectric properties of wood, Torgovnikov[12] suggested that the difference in dielectric properties of wood between the radial and tangential directions decreases with an increase in frequency above the microwave frequency range. This has, however, not been verified through experimentation.

In this paper, the attenuation and phase coefficients of hinoki (Japanese cypress), in longitudinal, radial, and tangential directions for quarter-sawn, flat-sawn, and cross-cut boards were evaluated while taking into account the effect of the anisotropy of the wood on its dielectric properties. A 100 GHz free electromagnetic wave, which is a representative frequency of a millimeter wave, was used on the basis of the behavior of the electromagnetic wave in wood as an orthotropic material. Furthermore, the dependency of the transmittance of the millimeter wave through hinoki in the grain direction was discussed by using the propagation theory with the attenuation and phase coefficients in order to examine the applicability of the propagation theory to wood.

Theory

Wood is generally orthotropic in permittivity, and the three principal axes of the anisotropy are the fiber direction (L), the radial direction (R), and the tangential direction (T). These three directions can be used to explain the permittivity of wood in an arbitrary direction. Let the principal axes of anisotropy correspond to the three rectangular coordinate axes (*X*, *Y*, *Z*) that describe the rectangular parallelepiped specimen. A millimeter wave is treated as a free electromagnetic wave that transmits in the *z* direction and that is polarized linearly in the *x* direction. The relationship between the coordinate axes for the electromagnetic wave and the specimen is shown in Fig. 1. By letting the *z*-axis be parallel to the *Z*-axis, the angle between the *x*- and *X*-axes, θ, is equal to that between the *y*- and *Y*-axes. Let the thickness of the specimen be d and the electric fields before and after the penetration through the specimen be E_0 and E, respectively. If the heterogeneity of a wood specimen such as the annual ring structure could be ignored, the transmittance, *P*, can be formulated by using Eq. 1[10],

$$P = \frac{|E|}{|E_0|} = t' \exp\left(-\frac{1}{2}\alpha_X d\right)\left|\cos^2\theta + \exp\left\{\frac{1}{2}(\alpha_X - \alpha_Y)d\right\}\exp\{j(\beta_X - \beta_Y)d\}\sin^2\theta\right|, \quad (1)$$

where α_X, α_Y, β_X, and β_Y are the attenuation and the phase coefficients in the *X* and *Y* directions, respectively; and t' is the product of the Fresnel transmission coefficients of the wood-to-air and air-to-wood interfaces and is regarded as a constant, though it depends on θ. If *x* is parallel or perpendicular to *X*, or θ is equal to 0° or 90°, Eq. 1 is rewritten as follows:

$$P_X = t' \exp\left(-\frac{1}{2}\alpha_X d\right) \quad (\theta = 0°) \text{ or} \tag{2}$$

$$P_Y = t' \exp\left(-\frac{1}{2}\alpha_Y d\right) \quad (\theta = 90°), \tag{3}$$

where P_X and P_Y are the transmittances in the X and Y directions, respectively. These equations imply that the dependences of P on d in the X and Y directions are affected by the attenuation coefficients in the X and Y directions, respectively.

Experimental

Apparatuses

The set-up for the millimeter wave transmitter and receiver system arranged in a coordinate system (x, y, z) is shown in Fig. 2. A Gunn diode was used to generate the millimeter wave at an average output power of 10 mW at 100 GHz. The output signal from the diode was modulated by a PIN-diode. The millimeter wave polarized linearly in the x direction was radiated in the z direction from a horn antenna and was transformed into a parallel beam using a plano-convex Teflon lens that is 50 mm in diameter and has a 50 mm focal length. The beam was focused onto a sensor with another plano-convex lens that was 50 mm in diameter and had a 100 mm focal length. The sensor received the electric field component parallel to the x direction. The received wave signal was processed in a lock-in amplifier (Stanford Research Systems Model SR850 DSP). The magnitude of the electric field of the millimeter wave was obtained as a voltage at the lock-in amplifier. The positions and the directions of the lenses in Fig. 2 were determined so that the gain of the millimeter wave reached maximum.

The distribution of the relative magnitude of the beam on the xy plane at positions (A) and (B) between the two plano-convex lenses (Fig. 2) is shown in Fig. 3. This distribution was obtained by scanning by using the sensor mentioned above on the xy planes at positions (A) and (B). Figure 3 shows that there is no significant difference in the distribution of the beam amplitude between (A) and (B) and a specimen set between (A) and (B) is irradiated on an area that was 40 mm in diameter with millimeter waves. It was confirmed that the distributions obtained at the positions other than (A) and (B) were almost the same as those in Fig. 3.

The transmittance of a millimeter wave was measured for wood specimens that were set between (A) and (B) in such a manner that their major faces were perpendicular to the beam. The transmittance P was estimated according to the right side of Eq. 1.

Specimens

Cross-cut (TR, parallel to TR plane), quarter-sawn (LR), and flat-sawn (LT) boards at nominal thicknesses of 0.2, 0.3, 0.5, 0.9, 1.5, and 2.0 cm were prepared from the heartwood of a hinoki (Japanese cypress, *Chamaecyparis obtusa*) wood under air-dry conditions (MC = 8 %). The quarter- and flat-sawn boards were cut from a piece of lumber, of which the average air-dry density was 347 kg/m^3, and the cross-cut boards were cut from another piece of lumber, 383 kg/m^3. The clear hinoki boards were used because they are straight-grained, show the small difference in density between early- and latewood, and adequately satisfy the assumption in theory that the heterogeneity of the specimen such as the annual ring structure was ignored.

As shown in Fig. 4, the annual ring deviation angle, θ_a, was defined as the angle between the tangential direction of the wood specimen and the direction of the electric field of the incident wave (x direction) for cross-cut boards, and the fiber deviation angle, θ_f, as the angle between the fiber direction and the x direction for quarter- and flat-sawn boards.

The principal axes X, Y, and Z (or z) of the anisotropy and the angle θ of the specimen mentioned in **Theory** correspond to T, R, L, and θ_a for cross-cut boards, L, R, T, and θ_f for quarter-sawn boards, and L, T, R, and θ_f for flat-sawn boards, respectively.

Measurement of transmittance

To examine the validity of the attenuation properties given by Eqs. 2 and 3, the transmittance P for each board of different thicknesses d was measured at θ = 0° and 180° and at θ = 90° and 270°, for cross-cut, quarter-sawn, and flat-sawn boards. Furthermore, to examine the validity of the anisotropy given by Eq. 1, the transmittance P was measured at intervals of 15° of the fiber deviation angle θ_f or the annual ring deviation angle θ_a from 0° to 360°.

Results and Discussion

Estimation of attenuation coefficient

Figures 5, 6, and 7 show the relations between the transmittance P and the thickness of specimen d for cross-cut, quarter-sawn, and flat-sawn boards, respectively. In these figures, $\ln(1/P^2)$ shows a good linear relationship to d for all boards, which is consistent with the theory shown as Eqs. 2 and 3. Some irregularities in Figs. 5-7 could be due to standing wave formation, which results from the interference between the incident and reflected waves, probably including the components of multiple

reflections. The fact the lines in Figs. 5-7 do not pass through the origin could be also due to the reflections. The slopes and intercepts of the regression lines in Figs. 5-7 were used to obtain the values of α and $\ln\left(1/t'^2\right)$ for each principal axis of the anisotropy, respectively (Figs. 8 and 9). Figure 8 shows that there is little difference in α_{L} between the quarter- and flat-sawn boards and that α_{R} and α_{T} are almost identical and smaller than α_{L}. The values of α_{R} and α_{T} for cross-cut boards are almost identical and larger than those for the quarter- and flat-sawn boards. This is probably due to the fact that the average air-dry density of cross-cut boards was larger than that of quarter- and flat-sawn boards. These findings support Torgovnikov's prediction[12] that the dielectric properties of wood in the radial and tangential directions would be identical above the microwave frequency range.

The ordinate intercepts of the regression lines, $\ln\left(1/t'^2\right)$, were almost the same for all boards without any significant differences (Fig. 9). This implies that the Fresnel transmission coefficient is little affected by the fiber direction, namely that the influence of the anisotropy of wood on the behavior of the electromagnetic wave is remarkably larger in the specimen than at the boundary between the specimen and the air. It is, however, not worth evaluating the absolute value t', since t' is affected by the component of the multiple reflection, a phenomenon that the millimeter wave reflects repetitively in a horn antenna to be used for the radiation and reception of the wave.

Dependency of transmittance on fiber direction and estimation of phase coefficient

Figures 10- 12 show the experimental and theoretical relations of the transmittance *P* to the annual ring deviation angle, θ_{a}, for cross-cut boards, to the fiber deviation angle θ_{f} for quarter- and flat-sawn boards, respectively. The theoretical relations for each board were obtained by substituting the parameters in Figs. 8 and 9 for those in Eq. 1. The difference between two phase coefficients, $\Delta\beta = \beta_X - \beta_Y$, was estimated as the value that minimizes the sum of the squares of the difference between the theoretical (P) and experimental (P') transmittances, $J(\Delta\beta)$ in Eq. 4, for cross-cut, quarter-sawn, and flat-sawn boards.

$$J(\Delta\beta) = \sum_i \sum_j \left| P'(d_i, \theta_j) - P(d_i, \theta_j, \Delta\beta) \right|^2 , \tag{4}$$

where d_i (i = 1, 2, ⋯ , 6) are the specimen thicknesses shown in Figs. 10-12, and θ_j (j = 1, 2, ⋯ , 25) are the fiber or annual ring deviation angles from 0° to 360° at intervals of 15°. To estimate $\Delta\beta$, which is a periodic function, from Eq. 4, the range of $\Delta\beta$

was supposed to be 0 to 10 rad/cm, since Reid *et al.*[10] reported 1.5 rad/cm for air-dry spruce at 100 GHz using a terahertz pulse wave. The estimated values of $\Delta\beta$ and the corresponding values of $J(\Delta\beta)$ are listed in Table. This table shows that the dielectric properties in the T and R directions are the same and different from those in the L direction. This is consistent with the findings for the attenuation coefficient α shown in Fig. 8 and Torgovnikov's predictions.

In Figs. 10-12, the plots of the experimental values of *P* against the fiber or annual ring deviation angles are shown together with the theoretical curves estimated from Eq. 1. For the quarter- and flat-sawn boards, the transmittance periodically and widely fluctuated against the fiber deviation angle θ_f, while for the cross-cut boards the transmittance was nearly constant over the entire annual ring deviation angle θ_a. These phenomena were theoretically the same as those for the transmission of linearly polarized visible rays through the 1/2 and 1/4 wave plates commonly used as optical elements[10]. In Figs. 11 and 12 the transmittances at 0° and 180° are smaller than at 90° and 270°. This is due to the fact that the attenuation coefficients in fiber direction are significantly larger than those in transverse direction (Fig. 8). Figures 11 and 12 also show that the transmittances at the intermediate angles are much smaller than the principal angles, particularly in lower two lines. This is due to the difference between two phase coefficients, $\Delta\beta = \beta_X - \beta_Y$, which is called birefringence[10]. This parameter is related to the difference in the propagation velocity of the electric field component of the wave between fiber and transverse directions.

Conclusion

The dielectric properties, attenuation and phase coefficients, and the transmittance were evaluated in terms of the anisotropy for hinoki, Japanese cypress, using free 100 GHz millimeter waves. The findings in this experiment were consistent with the general electromagnetic wave propagation theory for orthotropic materials.

Further examination is necessary to determine the dependency of the dielectric properties of wood on its moisture content, density, and temperature in the millimeter wave frequency range, because it has been reported that the dielectric properties depend on these properties of wood in the microwave frequency range,[13-15] which is the challenge to be solved in millimeter-wave frequency.

References

1. Eisele H, Haddad G (1998) Two-Terminal Millimeter-Wave Sources. IEEE Trans.

Microwave Theory Tech. 46:31-34

2. Volkov LV, Lyubchenko VE, Tikhomirov SA (1994) The arrays of GaAs antenna-coupled Schottky barrier diodes in millimeter wave imaging systems. Gallium Arsenide Applications Symposium. 97-100

3 .Goldsmith PF, Hsieh CT, Huguenin GR, Kapitzky J, Moore EL (1993) Focal Plane Imaging Systems for Millimeter-Wavelengths. IEEE Trans. Microwave Theory Tech. 41:1644-1675

4. Sheen DM, McMakin DD, Hall TE (2001) Three Dimensional Millimeter-Wave Imaging for Concealed Weapon Detection. IEEE Trans. Microwave Theory Tech. 49:1581-1592

5. Fujii Y, Fujiwara Y, Yanase Y, Okumura S, Narahara K, Nagatsuma T, Yoshimura T, Imamura Y (2007) Nondestructive Detection of Termites Using a Millimeter-Wave Imaging Technique. Forest Prod.J. 57:75-79

6. Peyskens E, de Pourcq M, Stevens M, Schalck J (1984) Dielectric properties of softwood species at microwave frequencies. Wood Sci. Technol. 18:267-280

7. Daian G., Taube A., Birnboim A., Shramkov Y., Daian M (2005) Measuring the dielectric properties of wood at microwave frequencies. Wood Sci. Technol. 39:215-223

8. James WL, Yen Y–H, King RJ (1985) A microwave method for measuring moisture content, density, and grain angle of wood. Research note FPL-0250

9. Schajer GS, Orhan FB (2005) Microwave Non-Destructive Testing of Wood and Similar Orthotropic Materials. Subsurface Sensing Technologies and Applications. 6:293-313

10. Reid M, Fedosejevs R (2006) Terahertz birefringence and attenuation properties of wood and paper. APPLIED OPTICS. 45:2766-2772

11. Oyama Y, Zhen L, Tanabe T, Kagaya M (2009) Sub-terahertz imaging of defects in building blocks. NDT&E International. 42:28-33

12. Torgovnikov GI (1993) Dielectric properties of Wood and Wood-Based Materials. Springer, Berlin. 196 pp

13. Norimoto M, Yamada T (1967) The Effect of Moisture Content on Modulus of

Rigidity and Dielectric Properties of Wood. Wood research: Bulletin of the Wood Research Institute, Kyoto University. 41:36-46

14. Norimoto M, Yamada T (1969) The Dielectric Properties of Wood II: Temperature Dependence of Dielectric Properties of Wood in Absolutely Dried Condition. Wood research: Bulletin of the Wood Research Institute, Kyoto University. 46:1-9

15. James WL (1975) Dielectric Properties of Wood and Hardboard: Variation with Temperature, Frequency, Moisture Content, and Grain Orientation. USDA Forest Service Research Paper. FPL-245

[Figure Legends]

Fig. 1. Relation between coordinate axes (*X*, *Y*, *Z*) of specimen and coordinate axes (*x*, *y*, *z*) of propagation of electromagnetic waves for quarter-sawn boards. The axes *X* and *Y* are parallel to the L and R directions, respectively.

Fig. 2. Experimental set-up for generation and detection of millimeter-waves arranged in coordinate system (*x*, *y*, *z*).

Fig. 3. Distribution of relative beam magnitude on *xy* plane at positions (A) and (B) in Fig. 2. The relative magnitude is the ratio of the *x* element of the electric field at a given point to that at the point where the maximum electric field appears.

Fig. 4. Relation between electric field direction, E_0, and principal axes of wood, L, R, and T, in coordinate system (*x*, *y*, *z*). θ_a, annual ring deviation angles; θ_f, fiber deviation angles.

Fig. 5. Relation between thickness of specimen *d* and $\ln(1/P^2)$ in T and R directions for cross-cut boards. *P*, transmittance of millimeter wave. Coefficients of determinations, R^2, are 0.963 and 0.956 for T and R directions, respectively.

Fig. 6. Relation between thickness of specimen *d* and $\ln(1/P^2)$ in L and R directions for quarter-sawn boards. *P*, transmittance of millimeter wave. Coefficients of determinations, R^2, are 0.974 and 0.965 for L and R directions, respectively.

Fig. 7. Relation between thickness of specimen *d* and $\ln(1/P^2)$ in L and T directions for

flat-sawn boards. *P*, transmittance of millimeter wave. Coefficients of determinations, R^2, are 0.979 and 0.902 for L and T directions, respectively.

Fig. 8. Attenuation coefficients for each principal axis of anisotropy for quarter-sawn, flat-sawn, and cross-cut boards.

Fig. 9. Intercepts of regression lines for each principal axis of anisotropy for quarter-sawn, flat-sawn, and cross-cut boards.

Fig. 10. Relation between θ_a and *P* for cross-cut boards with thicknesses of d_1 to d_6. Numerals in parentheses refer to measured board thicknesses in cm. The solid curves are drawn according to Eq. 1.

Fig. 11. Relation between θ_f and *P* for quarter-sawn boards with thicknesses of d_1 to d_6. Numerals in parentheses refer to measured board thicknesses in cm. The solid curves are drawn according to Eq. 1.

Fig. 12. Relation between θ_f and *P* for flat-sawn boards with thicknesses of d_1 to d_6. Numerals in parentheses refer to measured board thicknesses in cm. The solid curves are drawn according to Eq. 1.

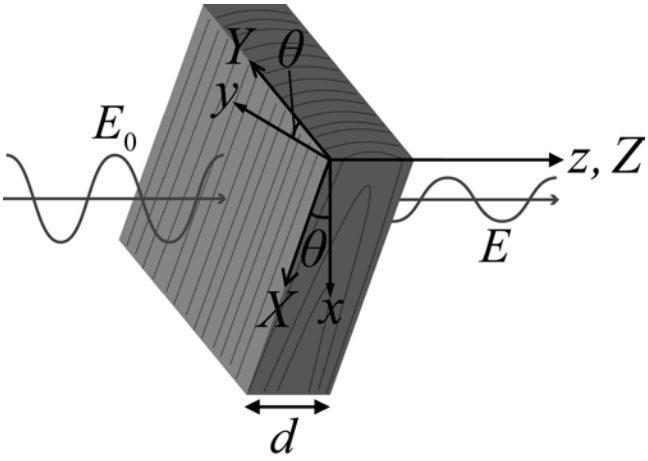

Fig. 1

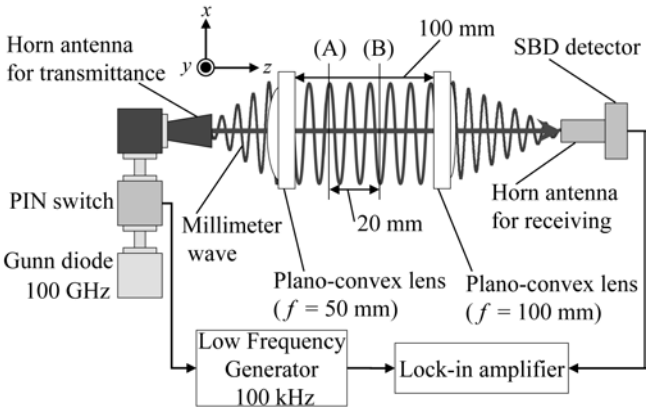

Fig. 2

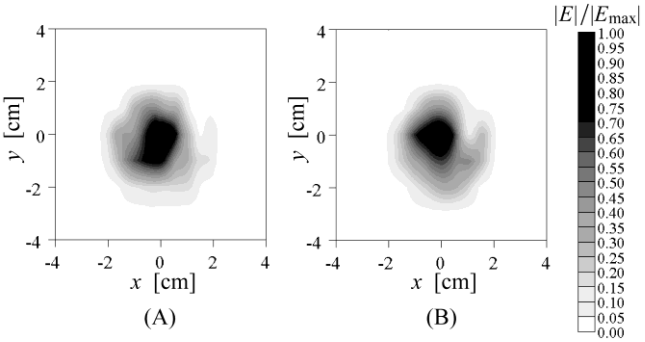

Fig. 3

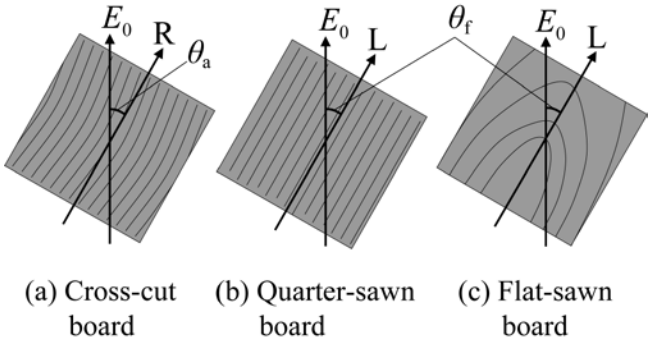

(a) Cross-cut board (b) Quarter-sawn board (c) Flat-sawn board

Fig. 4

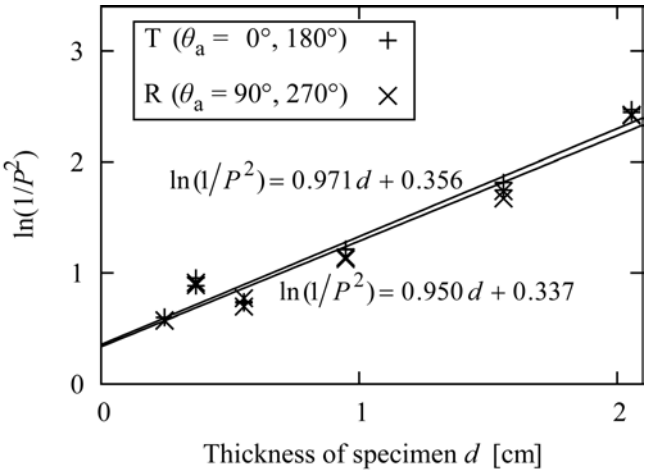

Fig. 5

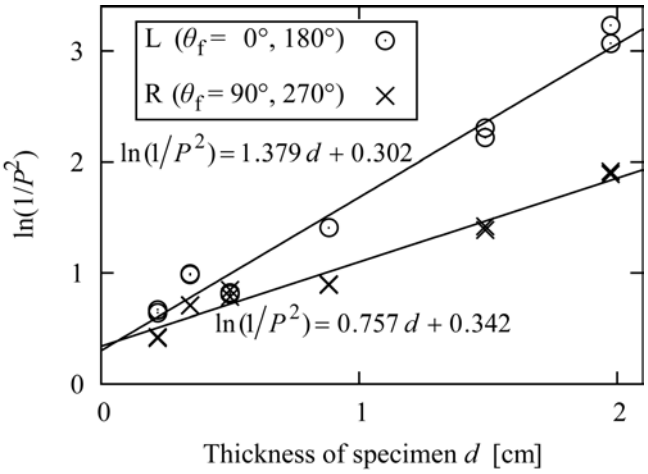

Fig. 6

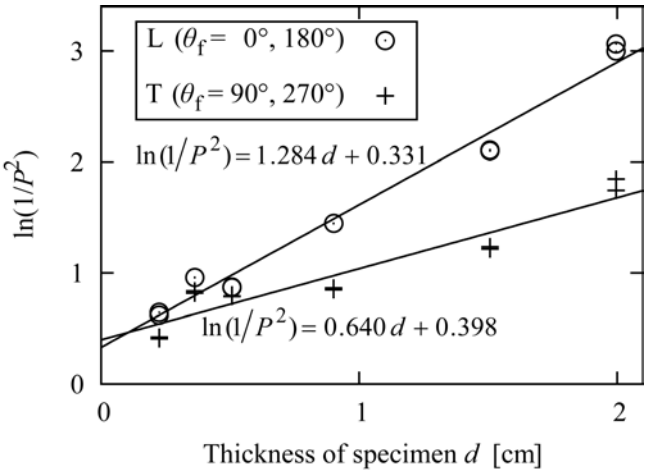

Fig. 7

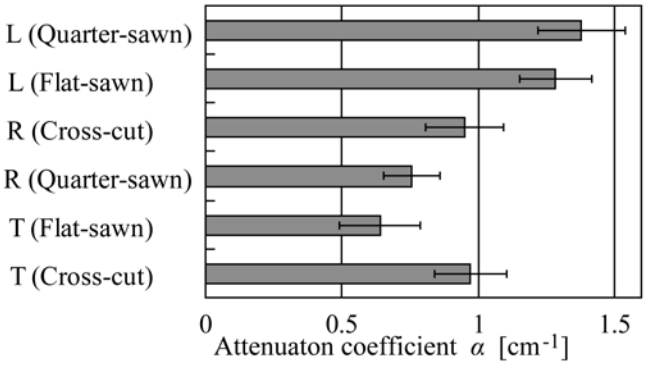

Fig. 8

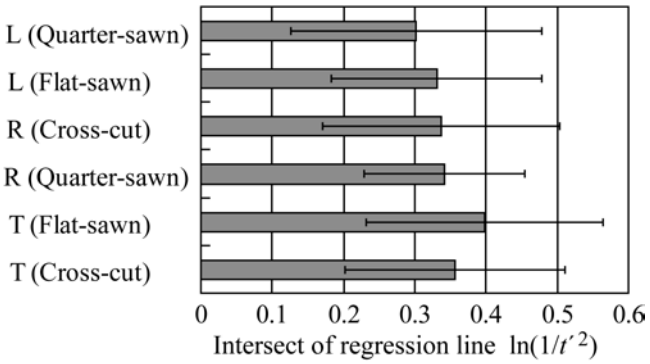

Fig. 9

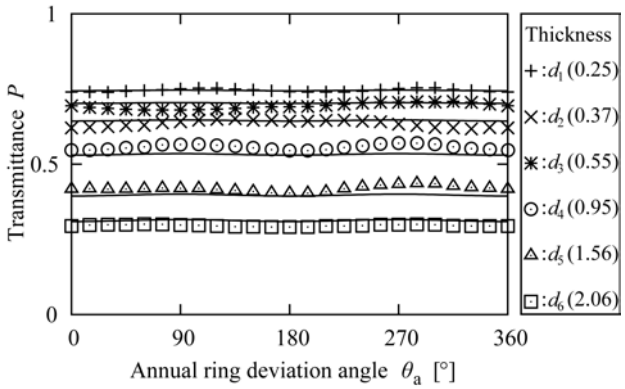

Fig. 10

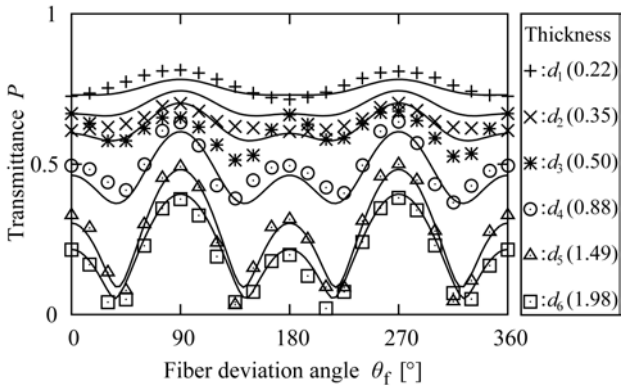

Fig. 11

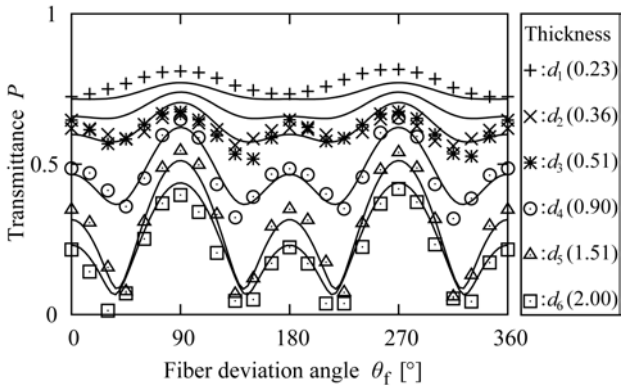

Fig. 12